Electrochemical Properties of Ruthenium-Based Nanocrystalline Materials as Electrodes for Supercapacitors

Patrick Soudan,[†] J. Gaudet,[‡] Daniel Guay,*[,‡] Daniel Bélanger,*[,†] and Robert Schulz[§]

Département de Chimie, Université du Québec à Montréal, C.P. 8888, succursale Centre-Ville, Montréal (Québec), Canada, H3C 3P8, INRS-Energie et Matériaux, 1650 Blvd. Lionel-Boulet, C.P. 1020, Varennes, Québec, Canada J3X 1S2, and Technologies Emergentes de Production et de Stockage, Institut de recherche d'Hydro-Quebec, 1800 Boul. Lionel-Boulet, Varennes, Quebec, Canada J3X 1S2

Received August 7, 2001

Nanocrystalline $Ti_xFe_yRu_zO_n$ materials were prepared by mechanical alloying using high-energy ball milling. The electrochemical properties of the materials were investigated in 1 M NaOH and 1 M H_2SO_4 aqueous solutions, using a composite electrode technology. The tested materials fall in two categories. On one hand, when the O/Ti ratio is larger than 1, Ru atoms are found in an hexagonal phase. Upon cycling in H_2SO_4 or NaOH, these materials exhibit a significant increase of their capacitance from ∼5 to ∼50 F/g. This is due to the progressive growth of a ruthenium oxide layer at the surface. On the other hand, when the O/Ti ratio is smaller than 1, Ru atoms are found in a cubic phase (CsCl), along with Ti and Fe atoms. In that case, the growth of a stable oxide phase at the surface of the material occurs only when it is cycled in basic electrolyte. The maximum attainable capacitance is also close to 50−60 F/g. The individual crystallites of as-milled nanocrystalline materials suffer from a strong tendency to agglomerate together. For example, it is shown that the electrochemically active surface area of nanocrystalline RuO_2 is only increased by a factor of 2 when the crystallite size is decreased from 600 to 15 nm, which amounts to a 40-fold increase of the specific surface area. Thus, higher surface area materials were obtained by performing an additional milling step with Al, which is followed by a subsequent leaching of Al with a NaOH solution. With that procedure, the best performances were obtained with leached Ti_2FeRuO_2, with a maximum capacitance of 110 F/g.

Introduction

In the past few years, many works have been devoted to materials for electrochemical supercapacitors.[1] Some of these materials exhibit almost rectangular capacitive cyclic voltammograms (CVs), which imply very rapid and reversible electrochemical processes. In particular, these conditions are achieved with activated carbons where essentially only charging of the double layer is involved. Some conducting polymers, such as polyaniline and polypyrrole, are also characterized by quasi-rectangular CVs. In this case, this pseudocapacitive behavior involves rapid insertion and diffusion of ions into the bulk of the polymer network.[1] These two kinds of materials are usable both in aqueous and nonaqueous media. Among materials usable only in aqueous solutions, ruthenium oxide distinguishes itself from other transition metal oxides by its exceptionally high charge storage capacity, due to high electronic and protonic conductivities, together with a high degree of reversibility of the redox processes which take place over a large potential range (up to 1.4 V).[1]

Previous investigations have allowed a better understanding of the origins of the high specific capacitance of ruthenium oxide.[1] It has been demonstrated that parameters such as the degree of hydration of the oxide (x in $RuO_2 \cdot xH_2O$) and its crystallinity play essential roles in determining the amount of charge exchanged during the redox processes and the shape of the CVs.[2,3,4] In the case of anhydrous crystalline materials obtained following a heat treatment at temperatures higher than 300 °C, the electrochemical capacitance as well as the HER activity increases when the dimension of the particles is reduced (i.e., the specific area is increased). Attempts to improve the performances of crystalline RuO_2 by decreasing the particle size has already been reported in the literature.[5] In the case of amorphous

* To whom correspondence should be addressed. E-mail: guay@inrs-ener.uquebec.ca daniel.belanger@uqam.ca.
[†] Université du Québec à Montréal.
[‡] INRS-Energie et Matériaux.
[§] Institut de recherche d'Hydro-Quebec.

(1) Conway, B. E. In *Electrochemical Supercapacitors: Scientific Fundamentals and Technological Applications*; Kluwer Academic/Plenum Publishers: New York, 1999. (b). Conway, B. E. *J. Electrochem. Soc.* **1991**, *138*, 1539.
(2) Zheng, J. P.; Jow, T. R. *J. Electrochem. Soc.* **1995**, *142*, L6.
(3) Zheng, J. P.; Cygan, P. J.; Jow, T. R. *J. Electrochem Soc.* **1995**, *142*, 2699.
(4) Jow, T. R.; Zheng, J. P. *J. Electrochem. Soc.* **1998**, *145*, 49.
(5) Wilde, P. M.; Guther, T. J.; Oesten, R.; Garche, J. *J. Electroanal. Chem.* **1999**, *461*, 154.

10.1021/cm010721c CCC: $22.00
Published on Web 02/09/2002

hydrated RuO_2, a similar reduction of the particle size does not yield an improvement in the performances of the material. This discrepancy is explained by the fact that redox reactions occur in the bulk of $RuO_2 \cdot H_2O$ whereas only the surface of the material is involved in the case of crystalline RuO_2.

Although ruthenium oxide allows the attainability of higher capacitance than all other oxide materials, the rarity of the metal and its very high cost as well as its probable toxicity have prompted researchers to identify compounds in which ruthenium could be replaced by cheaper elements. In this way, Wilde et al.[5] have been interested in ruthenate perovskites (e.g., $SrRuO_3$) and have obtained up to 160 F/g for a Raney-type oxide. Takasu et al.[6] reported interesting performances for RuO_2-VO_x electrodes prepared by dip-coating on Ti. Others oxides, such as TiO_2, SnO_2, or ZrO_2 have been mixed with RuO_2.[7,8,9,10,11] More recently, Jeong et al. reported the synthesis of mixed chromium−ruthenium oxides using soft chemistry (precipitation technique). These authors claimed an improvement of performances in comparison with RuO_2 for some particular compositions.[12]

In this work, we have attempted to evaluate the electrochemical characteristics of several nanocrystalline ruthenium-based materials with the intention of determining the influence of the other elements on the capacitance and the shape of the cyclic voltammograms. We will show how the initial structure of the material influences the oxide layer that grows at the surface of the material. The influence of the nanocrystalline state and of the specific area of the material on the capacitance will also be discussed.

Experimental Section

Materials. Nanocrystalline Ti−Ru−Fe−O powders were obtained by high-energy ball milling. A series of samples with various initial stoichoimetries were prepared. For simplicity, they will be referred to by their nominal composition. They were obtained by milling together pure metals (Ru, Ti, and Fe) and oxides (RuO_2, Ti_2O_3, TiO, and Fe_2O_3) purchased from Alpha (Johnson Matthey) and Anachemia. The purity of these powders was certified to be better than 99.9%. The interested readers will find a detailed description of the initial powder mixtures of each specific nanocrystalline Ti−Ru−Fe−O material elsewhere.[13] Most of the milling experiments were performed in WC vials with a modified Red Devil paint shaker mill (750 rpm). The volume of the crucibles was 40 mL. Two WC balls with diameters of 11 and 12.7 mm were used. The loading of the powder and all subsequent samplings were performed in a glovebox under an argon atmosphere. The crucibles were kept hermetically sealed with a Viton O-ring during milling. The initial charge was 5 g in all cases. The milling operation was performed during a period of 20−40 h. X-ray diffraction (XRD) histograms were obtained with a Siemens D-5000 diffractometer using Cu Kα radiation.

Chemicals. Acetylene black (Alfa, >99.9%, specific area = 80 m^2/g) and graphite (Alfa, conducting grade, −200 mesh) were dried at 100 °C under vacuum for 12 h before use. Dry PTFE was prepared from a 60% aqueous solution after removing water at 50 °C under vacuum and rinsing several times to eliminate the surfactant. 1 M H_2SO_4 and NaOH solutions were prepared from ACS grade reagents and deionized water (Barnstead Nanopure II).

Equipment. All experiments were performed in a beaker-type cell filled with electrolyte at ambient atmosphere. The working composite electrodes were made according to the procedure described below. The counter electrode was made of large area platinum gauze. The reference electrode was either a calomel electrode saturated with KCl (SCE) (H_2SO_4 electrolyte) or a Hg/HgO electrode (NaOH electrolyte). The electrochemical apparatus was composed of a potentiostat−galvanostat Solartron model 1287 operated under Corrware 2 software (Scribner Associates). The electrochemical characterization was performed using cyclic voltammetry (CV) at a scan rate of 10 mV/s. The capacitance was calculated from the mass of active material contained in the composite electrode (see below) and the lowest Coulombic charge that was obtained by integrating either the oxidative or reductive part of the CV over the potential window of the CV (which is generally 1.2 V).

Preparation of Composite Electrodes. To make electrodes based on powdered materials, it was decided to employ a composite electrode technology. This kind of electrodes are currently used in the industry of lithium batteries, since they are easy to handle due to the presence of PTFE which give them good mechanical properties. Moreover, the presence of graphite and acetylene black improves the electrical conductivity as well as the porosity of the electrode.

Powdered material (typically 30−80 mg) was first ground with acetylene black and graphite in an agate mortar. The mixture was then placed in a small beaker with dry PTFE, and the components were mixed in the presence of pure ethanol until a paste was obtained. Then, several successive rolling and folding procedures with ethanol on a glass plate resulted in a thin film (around 10−20 mg/cm^2) with good mechanical properties. After drying under vacuum at 50 °C to remove alcohol, the film was approximately composed of 80% active material, 7.5% acetylene black, 7.5% graphite, and 5% PTFE. It was then pressed between two stainless steel grids (AISI 304) under a pressure of about 5×10^2 MPa for 3 min. The dimension of the composite electrodes was generally close to 0.5 cm^2, with a mass of active material ranging between 3 and 12 mg. All the results shown herein have been reported to the mass of active material in the electrodes.

Commercial $RuO_2 \cdot 2H_2O$ was used to test the composite electrode technology used in this work. A capacitance value of 500 F/g was found for a potential window of 1.2 V. This value is similar to that obtained by Zheng et al[2,3,4] for a similar $RuO_2 \cdot 2H_2O$ material (530 F/g for a potential window of 1 V). Also, the shape of the CVs (not shown) is similar to that observed elsewhere for a similar material (see, for example, Figure 3 of ref 2). So, the composite electrode technology used in this work is a suitable and efficient way to test powdered electrode materials for supercapacitor applications.

Result and Discussion

A. Nanocrystalline Ti−Ru−Fe−O Compounds. Before discussing the electrochemical properties of nanocrystalline Ti−Ru−Fe−O compounds, let us first review what is known of their crystalline structure. According to the binary Ti−Fe and Ti−Ru phase dia-

(6) Takasu, Y.; Nakamura, T.; Ohkawauchi, H.; Murakami, Y. *J. Electrochem. Soc.* **1997**, *144*, 2601.
(7) Long, J. W.; Swider, K. E.; Merzbacher, C. I.; Rolison, D. R. *Langmuir* **1999**, *15*, 780.
(8) Takasu, Y.; Murakami, Y.; Minoura, S.; Ogawa, H.; Yahikozawa, K. In *Electrochemical Capacitors*; Delnik, F. M., Tomkiewicz, M., Eds.; PV 95−29, The Electrochemical Society Proceeding Series, Pennington, NJ, 1995; p 57.
(9) Ito, M.; Murakami, Y.; Kaji, H.; Yahikosawa, K.; Takasu, Y. *J. Electrochem. Soc.* **1996**, *143*, 32.
(10) Camara, O. R.; Trasatti, S. *Electrochim. Acta* **1996**, *41*, 419.
(11) Swider, K. E.; Merzbacher, C. I.; Hagans, P. L.; Rolison, D. R. *Chem. Mater.* **1997**, *9*, 1248.
(12) Jeong, Y. U.; Manthiram, A. *Electrochem. Solid-State Lett.* **2000**, *3*, 205.
(13) Yip, S.-H.; Guay, D.; Jin, S.; Ghali, E.; Van Neste, A.; Schulz, R. *J. Mater. Res.* **1998**, *13*, 1171.

Table 1. Physicochemical and Electrochemical Characteristics of Nanocrystalline $Ti_xFe_yRuO_n$ Compounds

formula	structure of Ru-containing material	wt % Ru	preparation	initial capacitance (F/g)	max capacitance (F/g)[a]	max e^- per Ru
$RuO_2 \cdot 2H_2O$	amorphous	59.8	commercial	500	500	1.05
$RuO_2 \cdot \epsilon H_2O$	RuO_2	76	heating of commercial $RuO_2 \cdot 2\ H_2O$ (600 °C, 3 h)	85	85	0.14
$Ti_{0.38}Fe_{0.24}RuO_{0.76}$	hcp-Ru	69.8	ball milling	5	30	0.054
$Ti_{0.15}Fe_{0.09}RuO_{0.58}$	hcp-Ru	82.5	ball milling	7	52	0.079
$Ti_{2.63}Fe_{1.23}O_2$	B2	0	ball milling	9	17	
Ti_2RuO_2	B2	44.2	ball milling	4	35	0.10
$Ti_{3.8}Fe_{2.37}RuO_{3.37}$	B2	21.5	ball milling	7	23	0.13
Ti_2FeRu	B2	40	ball milling	10	50	0.16
$Ti_2Fe_{2.14}RuO_2$	B2	29	ball milling	6	48	0.21
$Ti_2Fe_{1.25}RuO_2$	B2	33.9	ball milling	6	57	0.21
$Ti_{2.63}Fe_{0.63}RuO_2$	B2	34.4	ball milling	5	33	0.12
$Ti_{2.94}Fe_{0.31}RuO_2$	B2	34.7	ball milling	5	57	0.20
$Ti_2Fe_{0.33}RuO_{1.43}$	B2	42.4	ball milling	6	54	0.16
Ti_2FeRuO_2	B2	33.6	ball milling with Al followed by leaching	40	110	0.39

[a] After resting for several days in NaOH and/or after cycling.

grams,[14] pure Ti has an hexagonal structure with a low solubility limit for Fe and Ru (<1 at. % at all temperatures). At moderate temperature, Ti adopts a body-centered cubic (bcc) structure (β-Ti), whose solubility limit for Fe and Ru is in the range of 20 at. %. At equimolar concentration, both of these bcc structures exhibit an order−disorder transition and simple cubic TiFe and TiRu intermetallic compounds are formed, respectively. In these compounds, Ti is located on the 1a site (0, 0, 0) and Ru or Fe is located on the 1b site (1/2, 1/2, 1/2) of the cubic lattice.

As shown previously,[13,15,16,17,18] nanocrystalline Ti−Ru−Fe (without oxygen atom) is made almost exclusively (97 wt %) of a cubic phase, whose stoichiometry is Ti_2RuFe. Upon the addition of oxygen, Ti reacts to form stable titanium oxides. As a result, the amount of (metallic) Ti that can dissolve Ru or Fe atoms decreases. This translates into the formation of Ti-depleted cubic phase.[16,17] Also, since Fe has a larger tendency than Ru to dissolve in β-Ti, the excess Ru appears as an hexagonal phase in nanocrystalline compounds that have a large O/Ti ratio. So, the nanocrystalline compounds investigated here will be classified in two different categories. In the first one, O/Ti > 1 causes Ru to appear as an hexagonal phase, while in the second one, O/Ti < 1 leads to Ru atoms being dissolved in the β-Ti phase. In all cases, the materials obtained after ball milling are composed of nanocrystallites of the order of 10 nm.[15,16,18] Keeping that in mind, we can now look at the electrochemical behavior of nanocrystalline Ti−Ru−Fe−O compounds (see Table 1).

A.1. Nanocrystalline Compounds with Ru in an Hexagonal Phase. Nanocrystalline Ti−Ru−Fe−O with $Ti_{0.38}Fe_{0.24}RuO_{0.76}$ and $Ti_{0.15}Fe_{0.09}RuO_{0.58}$ has been tested. Since O/Ti > 1, Ru exists mainly as an hexagonal phase. The CVs of these two compounds exhibit very poor capacitive behavior, since their shape is far from rectangular. The CVs obtained in H_2SO_4 are presented in Figure 1 for $Ti_{0.38}Fe_{0.24}RuO_{0.76}$. A similar CV is obtained for $Ti_{0.15}Fe_{0.09}RuO_{0.58}$. The capacitance values are 5 and 7 F/g for $Ti_{0.38}Fe_{0.24}RuO_{0.76}$ and $Ti_{0.15}Fe_{0.09}RuO_{0.58}$, respectively (Table 1). Such values are low and are essentially due to (i) the Coulombic charge involved at the beginning of the H-adsorption process at potentials below 0 V during the negative potential scan and (ii) an unidentified oxidative processes occurring above 0.8 V during the positive scan (Figure 1, curve A). A similar oxidative process was observed in the first CVs of pure nanocrystalline Ru prepared by ball milling.[19]

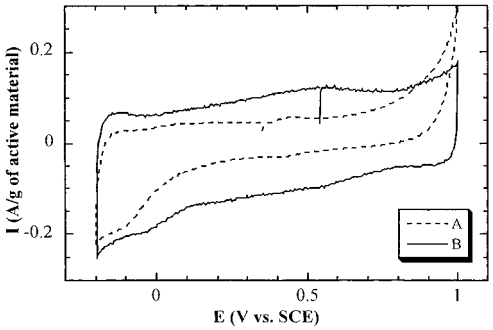

Figure 1. Continuous cyclic voltammetry (scan rate: 10 mV/s) of nanocrystalline $Ti_{0.38}Fe_{0.24}RuO_{0.76}$ in aqueous 1M H_2SO_4: (A) 3rd cycle and (B) 200th cycle.

Despite the negligible capacitance observed during the first few cycles, it is interesting to note that a capacitive behavior progressively appears upon continuous cycling in acidic solution, leading to an increase of the capacitance. Thus, a capacitance of 10 F/g is reached after 200 cycles in the case of $Ti_{0.38}Fe_{0.24}RuO_{0.76}$ (Figure 1, curve B) and 22 F/g after 60 cycles in the case of $Ti_{0.15}Fe_{0.09}RuO_{0.58}$ (not shown), corresponding to 0.018 and 0.034 e^- per Ru, respectively. This increase of capacitance must be related to the growth of an oxide film at the surface of hexagonal Ru. The progressive growth of an oxide film with potential cycling at hexagonal Ru, accompanied by a concomitant increase of the capacitive reversible current response, has already been observed in the past (for example, see ref 1[20]). Consistently, the material that presents the higher

(14) Massalski, T. B., Murray, J. L., Bennett, L. H., Baker, H., Eds.; *Binary Alloy Phase Diagrams*, 2nd ed.; ASM Int.: Materials Park, OH, 1990.
(15) Blouin, M.; Guay, D.; Huot, J.; Schulz, R. *J. Mater. Res.* **1997**, *12*, 1492.
(16) Blouin, M.; Guay, D.; Huot, J.; Schulz, R.; Swainson, I. P. *Chem. Mater.* **1998**, *10*, 3492.
(17) Blouin, M.; Schluz, R.; Bonneau, M. E.; Bercier, A.; Roué, L.; Guay, D.; Swainson, I. P. *Chem. Mater.* **1999**, *11*, 3220.
(18) Blouin., M.; Guay, D.; Schulz, R. *J. Mater. Sci.* **1999**, *34*, 5581.
(19) Roué, L.; Blouin, M.; Guay, D.; Schulz, R. *J. Electrochem. Soc.* **1998**, *145*, 1624.
(20) Hadzi-Jordanov, S.; Kozlowska, H. A.; Conway, B. E. *J. Electroanal. Chem.* **1975**, *60*, 359.

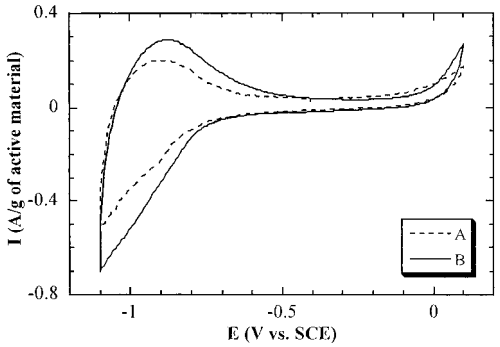

Figure 2. Cyclic voltammograms (scan rate: 10 mV/s) of nanocrystalline $Ti_{2.63}Fe_{1.23}O_2$ in aqueous 1M NaOH: (A) before and (B) after resting in NaOH for 7 days.

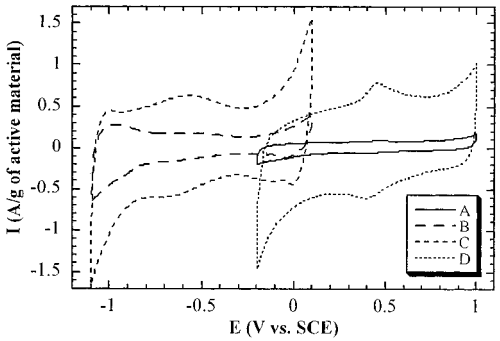

Figure 3. Cyclic voltammograms (scan rate: 10 mV/s) of nanocrystalline $Ti_2Fe_{1.25}RuO_2$: (A) pristine electrode in 1M H_2SO_4, (B) in 1M NaOH after 50 cycles in 1M NaOH, (C) in 1M NaOH after resting 4 days in 1M NaOH, and (D) in 1M H_2SO_4 after resting in 1M NaOH.

capacitance and especially the higher and faster increase of capacitance during cycling is the one that is the richest in Ru. After the electrodes have rested in 1 M NaOH for several days, the capacitance values of $Ti_{0.38}Fe_{0.24}RuO_{0.76}$ and $Ti_{0.15}Fe_{0.09}RuO_{0.58}$ increase to 30 and 52 F/g, respectively, corresponding to 0.054 and 0.079 e^- per Ru (Table 1). This indicates that some modification and reorganization of the previously grown oxide layer takes place.

As expected, the behavior of Ru-free nanocrystalline compound significantly differs from that of the previous materials. The CVs of nanocrystalline $Ti_{2.63}Fe_{1.23}O_2$ in 1M NaOH are presented in Figure 2. The CVs are not purely capacitive, indicating a charge storage mechanism different from those containing Ru or RuO_2 species. Unlike the previous two samples, there is practically no change in the shape of the CVs or in the capacity of the material even after a stay of 7 days in a basic electrolyte. Similar observations are made when H_2SO_4 is used instead of NaOH. These results confirm that the higher capacity and the change observed in the CVs of Ru-containing nanocrystalline materials are due to the transformation of part of Ru into $RuO_2 \cdot xH_2O$.

A.2. Nanocrystalline Compounds with Ru in a Cubic Phase. Several nanocrystalline Ti−Ru−Fe−O materials with O/Ti < 1 were prepared and tested. These are Ti_2RuO_2, $Ti_{3.8}Fe_{2.37}RuO_{3.37}$, Ti_2FeRu, $Ti_2Fe_{2.14}RuO_2$, $Ti_2Fe_{1.25}RuO_2$, $Ti_{2.63}Fe_{0.63}RuO_2$, $Ti_{2.94}Fe_{0.31}RuO_2$, and $Ti_2Fe_{0.33}RuO_{1.43}$ (see Table 1). In these materials, most of Ru exists as solute atoms in the cubic structure of β-Ti. The shape of the CVs for the pristine electrodes resembles that shown in Figure 3 for $Ti_2Fe_{1.25}RuO_2$ (curve A). They are characterized by the same low initial capacitance (4−10 F/g), which corresponds to about 0.01−0.04 e^- per Ru (see Table 1). For all these materials, it is observed that the initial capacitance remains almost unchanged after either cycling in 1 M H_2SO_4 or resting several days in this electrolyte. This behavior is markedly different from that observed in the previous section, where a systematic increase of the capacitance values was found when the electrode material was continuously cycled in an acidic solution. It indicates that the growth of a stable ruthenium oxide layer at the surface of nanocrystalline compounds with Ru in a cubic phase is prevented in acidic solution. This is thought to arise as a consequence of (i) the solubility of the oxidation products of the Ti and Fe metal ions found in the cubic phase and (ii) the low density of Ru atoms in the cubic phase.

The capacitance of nanocrystalline Ti−Ru−Fe−O materials with O/Ti < 1 can however be substantially increased by cycling in 1M NaOH. For example, as illustrated in Figure 3, an increase by a factor of 3, leading to a capacitance of 18 F/g, was achieved with $Ti_2Fe_{1.25}RuO_2$ after 50 cycles in 1M NaOH (curve B). In this case, the oxide and hydroxide that are formed upon oxidation of Fe and Ti are less soluble in the electrolyte, thereby contributing to the stability of the ruthenium oxide layer that grows upon cycling.

A still higher increase was achieved by simply leaving the electrode several days in the alkaline solution, as is indicated in Table 1 by the maximum capacitance reached by these materials. As an example, a capacitance of 57 F/g was attained in the case of $Ti_2Fe_{1.25}RuO_2$ after it was rested for 4 days in 1M NaOH (see Figure 3, curve C). Again, this would indicate that some modification and reorganization of the previously grown oxide layer takes place. This increase of capacitance is maintained after it is returned into 1M H_2SO_4, since 55 F/g is recovered in the case of $Ti_2Fe_{1.25}RuO_2$ (see Figure 3, curve D).

We must also notice that this last CV displays a set of redox waves in the potential region close to 0.4−0.5 V that are reminiscent of those observed when fully hydrated ruthenium oxide is cycled. This indicates that the composition of the ruthenium oxide layer at the surface of these nanocrystalline compounds is close to $RuO_2 \cdot 2H_2O$, in contrast to what is observed in the case of Ru-rich compounds (compare Figures 1 and 3). A similar behavior was observed in the case of $RuO_2 \cdot xH_2O$ generated at a Ti electrode in a solution containing $RuCl_3$ using repetitive CVs to first reduce Ru(III) into Ru during the negative scans and then to oxidize Ru into RuO_2 during the positive scans.[21] Owing to the low surface density of Ru atoms, less dense and more hydrated $RuO_2 \cdot xH_2O$ oxide film would grow in these conditions, explaining the presence of very distinctive redox peaks in the CVs. A similar explanation must hold in the present case, since the minimum distance between Ru−Ru atoms in the cubic phase structure is ~3 Å, much larger than the distance of closest approach in hexagonal Ru. The presence of oxides and hydroxides of Ti and Fe must also contribute to this effect.

B. Influence of the Nanocrystallinity on the Capacitance. The specific area of nanocrystalline Ti−

(21) Hu, C. C.; Huang, Y. H. *J. Electrochem. Soc.* **1999**, *146*, 2465.

Ru−Fe−O prepared by high-energy ball milling is quite low, of the order of a few square meters per gram, even if these compounds are made of crystallites with size of the order of a few nanometers. In these materials, the crystallites are agglomerated into larger grains, which tend to decrease the specific area. Nevertheless, it was hoped that the numerous grain boundaries found in the material would act as fast diffusion paths for the small H_3O^+ and OH^- ions involved in the redox processes, thereby causing a marked increase of the capacitance value as the crystallite size gets smaller and smaller.

To verify the previous assertion, the capacitive behavior of well-crystallized and dehydrated RuO_2 was compared to its nanocrystalline counterpart. Dehydrated RuO_2 was chosen instead of hydrated $RuO_2 \cdot xH_2O$, since the capacitance of the former material increases with its specific area, while that of the latter is more sensitive to the water content. Any change in the capacitive behavior of nanocrystalline dehydrated RuO_2 should therefore reflect a modification of the electrochemically accessible surface area.

To perform these measurements, commercial $RuO_2 \cdot xH_2O$ powder was first dehydrated at 600 °C for more than 10 h in an open furnace. The X-ray diffractogram of the resulting powder shows only the characteristic diffraction peaks of RuO_2. These peaks are sharp, indicating that the crystallite size is large. An estimation of the crystallite size from the width of the diffraction peak using the Debye−Scherrer formula yields >600 nm. This material was then milled for 40 h. The X-ray diffractogram of the resulting powder closely resembles that of the starting material, except for the fact that the diffraction peaks are broader. After milling the crystallite size is ∼15 nm.

The comparison between the electrochemically active surface areas of crystalline and nanocrystalline RuO_2 was performed according to a procedure developed by Trasatti.[22] It involves the calculation of the voltammetric charges as a function of the sweep rates. As observed with conducting oxide electrocatalysts prepared by thermal decomposition,[23,24] the voltammetric charge (q^*) decreases as the potential scan rate (ν) is increased (Figure 4). In the case of a reversible redox transition, the dependence of q^* on ν is usually explained by the slow diffusion of protons into pores, cracks, and grains boundaries. At a high sweep rate, diffusion limitation slows the accessibility of protons to the inner surface of the electrode material. The electrochemical response then depends only on the outer active surface, where diffusion of protons is not hampered. The extrapolation of q^* to $\nu = \infty$ from the q^* vs $\nu^{-1/2}$ plot (Figure 4, upper panel) gives the outer charge, q_O^*, which is related to the outer and more accessible active surface. At a low sweep rate, protons have enough time to diffuse to the inner and less accessible active surface. The extrapolation of q^* to $\nu = 0$ from the 1/q* vs $\nu^{1/2}$ (Figure 4, lower panel) gives the total charge, q_T^*, which is related to the whole active surface. The difference between q_T^* and

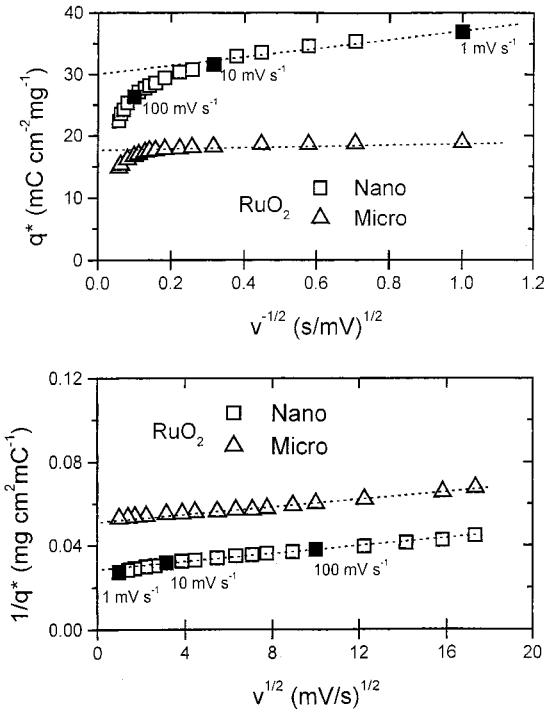

Figure 4. Variation of the voltammetric charge (q^*) with respect to the sweep rates.

q_O^* gives q_I^*, the charge related to the inner and less accessible active sites. In the case of micro- and nanocrystalline RuO_2, $q_T^* = 20$ and 35 C cm $^{-2}$ g^{-1}, while $q_O^* = 17$ and 29 C cm^{-2} g^1, respectively. A measure of the material porosity can be obtained by computing q_I^*/q_T^*. In the case of micro- and nanocrystalline RuO_2, these ratios are almost identical at 0.18 and 0.20, respectively. The boundaries created in the nanocrystalline material during the milling process are not readily accessible to protons.

As seen above, the variation of the electrochemically active surface area (q_T^*) when the crystallite size is reduced from 600 to 15 nm is less than a factor of 2. A simple calculation of the surface area, based on the crystallite size and on the assumption that the surface of each crystallite is readily accessible, yields values of 0.35 and 14 m^2 g^{-1} for micro- and nanocrystalline RuO_2, respectively. Assuming again that the surface of each crystallite is accessible to protons, this would translate to a 40-fold increase of q_T^*. The discrepancy between both sets of results obviously points to the fact that the grain boundaries of nanocrystalline RuO_2 do not act as fast diffusion paths for protons. It can be understood by looking at the microstructural organization of the nanocrystalline material. In these materials, crystallites with nanometer dimensions are agglomerated into larger grains, causing the electrochemically active surface area to be much smaller than expected. Thus, specific procedures need to be developed to reduce the agglomeration of crystallites.

C. Behavior of Leached Material. It was decided to apply a recently developed leaching process to the nanocrystalline $Ti_xFe_yRu_zO_n$ materials studied here to increase their specific areas and their capacitive behavior. Briefly, the process consists of adding Al to the elements used to prepare the compounds.[25,26] At the end of the milling process, Al is dissolved in a basic solution

(22) Baronetto, D.; Krstajié, N.; Trasatti, S. *Electrochim. Acta* **1994**, *39*, 2359.
(23) Ardizzone, S.; Fregonara, G.; Trasatti, S. *Electrochim. Acta* **1990**, *35*, 263.
(24) De Pauli, C. P.; Trasatti, S. *J. Electroanal. Chem.* **1995**, *396*, 161.

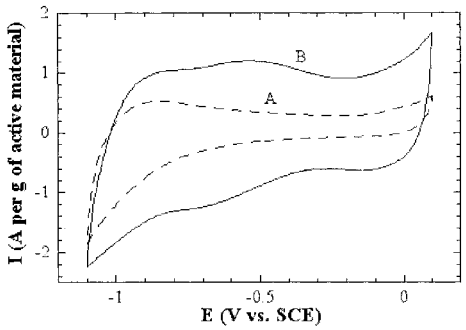

Figure 5. Cyclic voltammograms (scan rate: 10 mV/s) of leached nanocrystalline Ti_2FeRuO_2 in 1M NaOH: (A) pristine electrode and (B) the same electrode after cycling and resting in 1M NaOH.

(NaOH), leading to a nanocrystalline material with a larger surface area. This process is similar to that used to prepare Raney-nickel, where caustic leaching of $NiAl_3$ alloy is performed.[27] With the use of this procedure, close to a 10-fold increase of the specific area has been obtained. The residual Al content of the leached materials is low and corresponds to a small fraction of Al atoms embedded in the cubic phase of the material.[25,26]

The procedure described above could not be applied to RuO_2, since an oxido-reduction reaction between RuO_2 and Al could take place during the milling operation.[28,29] The leaching process has thus been used directly on nanocrystalline $Ti_xFe_yRu_zO_n$. The CVs of leached nanocrystalline Ti_2FeRuO_2 recorded in 1M H_2SO_4 (not shown) give an initial capacitance of 40 F/g (see Table 1), which is a factor that is higher by 7−8 than that of the same material prepared previously (see section A.2). The observed increase of the initial capacitance of the material is directly related to the larger specific area of the leached material.

As expected from the results of section A.2, the capacity of the leached material remains stable when it is cycled in H_2SO_4. On the contrary, the CVs on Figure 5 show that the capacitance in 1M NaOH, which is initially equal to 40 F/g, is increased to 110 F/g during cycling and resting (1 day or more) in this basic solution. The same capacity (110 F/g) is found when the electrode is returned into an H_2SO_4 electrolyte. The characteristic redox peaks at 0.4−0.5 V are then observed, confirming that the grown ruthenium oxide layer is hydrated. As far as we can tell, leached nanocrystalline Ti_2FeRuO_2 behaves exactly like the nonleached material, except for the initial increase of capacity.

Conclusion

Nanocrystalline $Ti_xFe_yRu_zO_n$ materials prepared by high-energy ball milling exhibited a low initial capacitance (4−10 F/g) in either 1M H_2SO_4 or 1M NaOH aqueous solutions. In the case of materials that contains metallic Ru, a significant increase of the pseudocapacitive behavior is found when the electrode is cycled in either acidic or basic electrolytes. This is due to the growth of an active $RuO_2{\cdot}xH_2O$ layer at the surface of the material. In the case of materials where Ru is imbedded in a cubic phase (along with Ti and Fe atoms), the growth of an active and stable $RuO_2{\cdot}xH_2O$ layer in acidic electrolyte is hampered. This is thought to be due to the solubility of Ti and Fe oxidation products and the low surface density of Ru atoms. These results demonstrate that the electrochemical behavior of the matrixes used to dilute ruthenium is crucial in determining the pseudocapacitive behavior of the resulting materials.

Finally, our results clearly demonstrate that the high surface area of nanocrystalline materials is not completely electrochemically accessible. To achieve a larger electrochemically accessible surface area, it will be essential to develop specific procedures to reduce the agglomeration of crystallites or to synthesize materials having faster ionic diffusion paths that will allow access to the bulk of the materials at a faster switching rate.

Acknowledgment. The Fonds pour la Formation de Chercheurs et l'Aide à la Recherche (FCAR) funded this research. We also wish to acknowledge M. Preda (Département des Sciences de la terre, UQAM) for the XRD experiments, and the financial contribution of UQAM and INRS-Énergie et Matériaux.

CM010721C

(25) Razafitrimo, H.; Blouin, M.; Roué, L.; Guay, D.; Schulz, R. *J. Appl. Electrochem.* **1999**, *29*, 627.
(26) Razafitrimo, H.; Blouin, M.; Roué, L.; Guay, D.; Huot, J.; Schulz, R. *J. Metastable and Nanocryst. Mater.* **1999**, *2*−*6*, 513.
(27) Wendt, H.; Plzak, V. In *Electrochemical Hydrogen Technologies: electrochemical production and combustion of hydrogen*; Wendt, H., Ed.; Elsevier: Amsterdam, 1990; pp 15−62.
(28) Blouin, M.; Guay, D.; Schulz, R. *J. Mater. Sci.* **1999**, *34*, 5581.
(29) Schaffer, G. B.; Cormick, P. G. *J. Mater. Sci. Lett.* **1990**, *9*, 1014.